6901

A CONTROL STRATEGY FOR A VARIABLE AIR VOLUME SYSTEM

M. Zaheer-uddin[1] and P. A. Goh[2]

Abstract

A multi-input, multi-output control strategy for a variable air volume system is developed. The control variables are the coil face and bypass damper opening fractions and the input energy required to run the chiller. The model outputs are the zone dry bulb temperature and the relative humidity.

The overall model consists of sub-models for the zone loads, the cooling and dehumidifying coil, the chiller and storage tank arrangement, a fan and associated ductwork. The model equations are described and the controller algorithms for implementation are given. In order to implement the control strategy the steady-state optimal values for supply air enthalpy and the chilled water temperature are required. A method of computing these values is given. The operating performance of the VAV system is illustrated using several simulated test cases. The results indicate that the controllers are responding to changing loads in a stable and efficient manner. This is shown in terms of time response characteristics of the controllers to a step change in load and as well as to a typical daily load profile. In both cases, the control strategy is able to maintain the zone dry bulb temperature and relative humidity close to the set point values.

---

1 M. Zaheer-uddin, Assistant Professor, Centre for Building Studies, Concordia University, 1455 de Maisonneuve Blvd. W., Montreal, Quebec, Canada H3G 1M8

2 P. A. Goh, Graduate Student, Centre for Building Studies, Concordia University, Montreal, Quebec, Canada H3G 1M8.

A CONTROL STRATEGY FOR A VARIABLE AIR VOLUME SYSTEM

M. Zaheer-uddin and P. A. Goh

1. Introduction

Central heating, ventilating and air conditioning (HVAC) systems are broadly classified into two categories, namely, constant volume (CV) systems and variable air volume (VAV) systems [1]. Constant volume systems, as their name implies, supply constant quantity of conditioned air to the space and the condition of the supply air (dry bulb temperature and humidity ratio) is varied in response to the changing loads. Thus, the CV systems are well suited when the load characteristics of different spaces are the same (for example, single zone systems). On the other hand, since different spaces in large buildings are subjected to different loads at any given time, the single zone CV systems can not supply conditioned air at different temperatures to suit the needs of individual zones. Under these circumstances multi-zone CV systems are used.

One draw back of the CV systems (single or multi-zone) is that the fan energy consumption remains the same irrespective of the zone loads. An alternative system which provides the supply air to different zones according to their needs while at the same time uses less fan energy at low loads is known as VAV system. These systems are capable of supplying varying quantities of air to different zones. Since the quantity of supply air is proportional to the fan speed and fan power is proportional to cube of the speed, it is evident that at low loads only low quantities of air are required and hence considerable amount of fan energy could be saved.

Although VAV systems have definite advantages in reducing the operating costs, they are also known to be difficult to control. One problem is that when the supply air quantities are reduced in response to decreasing load, the relative humidity of the air tends to be high unless additional control actions are taken. Furthermore, low air flow rates may lead to thermal discomfort due to inadequate air movements and poor indoor air quality which could be attributed to low ventilation rates. Under these circumstances the issue of designing control strategies for VAV systems become quite important.

There have been some studies done concerning the control of VAV systems. For example, reference 2 deals with the practical issues of the admitting outdoor air independent of VAV fan dynamics. Designing and tuning of PI controllers to control the discharge air temperature is discussed in [3,4,5]. Experimental studies on implementation of adaptive controllers in HVAC systems are discussed in reference 6. Bypass control and its effect on humidity control in a conditioned space is studied in reference 7. However, these studies deal with air-side loop control problems. What is not addressed though is the minimization of chiller energy when the chiller is an integral part of the VAV system. In this paper, we address the performance of a VAV system based on not only the control of supply air conditions but also the energy used by the chiller. Control strategies based on such dual performance criterion will be superior.

In the following, the physical model of the VAV system used in this study will be described and mathematical models of the component systems and the overall system will be developed (section 2). The control strategy will be developed in section 3. Implementation of the control strategy and the results obtained through computer simulation runs will be presented in section 4. Conclusion will be given in section 5.

2. The Model

Figure 1 shows the schematic diagram of the VAV system used in this study. The major elements of the system are i) a single zone environmental space, ii) a cooling and dehumidifying coil, iii) a chiller and a storage tank iv) face and bypass dampers, v) a fan vi) ductwork and vii) a feedback control system. The operation of VAV system can be understood by tracing the path of air around the loop.

For example, the air from the zone returns through the return duct, a portion of this air is exhausted and the remaining air is mixed with the fresh outside air. This mixed air which is hot and humid (considering cooling case) is cooled and dehumidified in the cooling coil. The cooling coil receives chilled water from the chiller and storage tank arrangement shown in the figure. The air leaving the coil must be at appropriate conditions (in terms of dry bulb temperature and humidity ratio) in order to satisfy the cooling load requirements of the zone. Therefore, for a good control of zone air temperature and humidity ratio, the supply air conditions must be continuously modulated. This is accomplished by the feedback control system (broken lines in Fig. 1).

As shown in the figure there are three control variables that can be varied in order to improve the overall performance. For example, the quantity of supply air is controlled by increasing or decreasing the fan speed. The condition of the air leaving the coil is controlled through a combination of face and bypass damper setting and by controlling the temperature of the chilled water flowing in the cooling coil. A third control action deals with the regulation of input energy required to run the chiller as a function of cooling load.

All these three control actions require feedback signals from the room thermostat (T) and the humidity sensor (W). When the room temperature increases because of an increase in cooling load, the difference between the setpoint and the actual values of the outputs (temperature and humidity ratio) increases. This is known as error which is fed back to the controllers in order to initiate the control action. Typically in this case (that is when the cooling load increases) i) the fan speed is increased to increase the mass flow rate of supply air ii) the bypass dampers are partially closed and hence the face dampers are opened so that a higher fraction of air passes through the cooling coil iii) the chiller energy consumption is controlled such that it is just sufficient to meet the increased cooling load. It must be noted that all three control actions are coupled in the sense the action of one influences the other. Therefore, the effect of changing loads on the overall performance of the system must be carefully incorporated into the control strategy.

2.1 Analytic Formulation

If m_a is the mass flow rate, h_s and W_s are the enthalpy and humidity ratio of the supply air an enthalpy balance on a single zone environmental space (Fig. 2) is written

$$m_a (h_z - h_s) = \Sigma q_s + \Sigma m_w h_w + q_{aux} \tag{1}$$

where the rate of heat extracted from the supply air is equated to the sum of all sensible loads (Σq_s), latent loads ($\Sigma m_w h_w$) and terminal reheat energy q_{aux} added, if any. Similarly, a moisture balance on the zone gives

$$m_a (W_z - W_s) = m_w \tag{2}$$

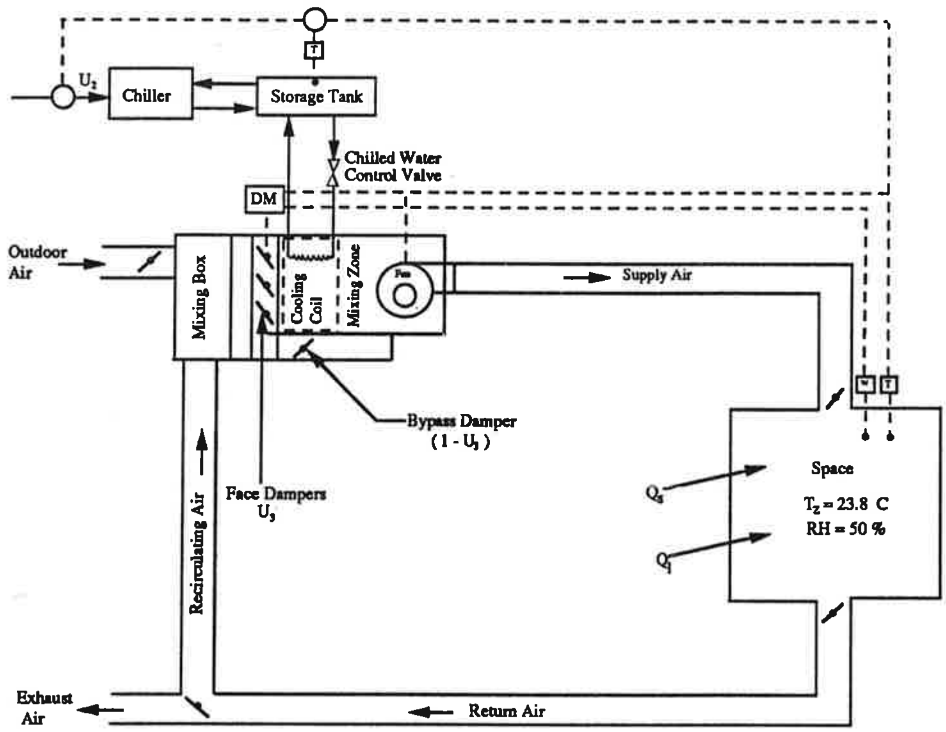

Figure 1 Schematic Diagram of a Variable Air Volume (VAV) System

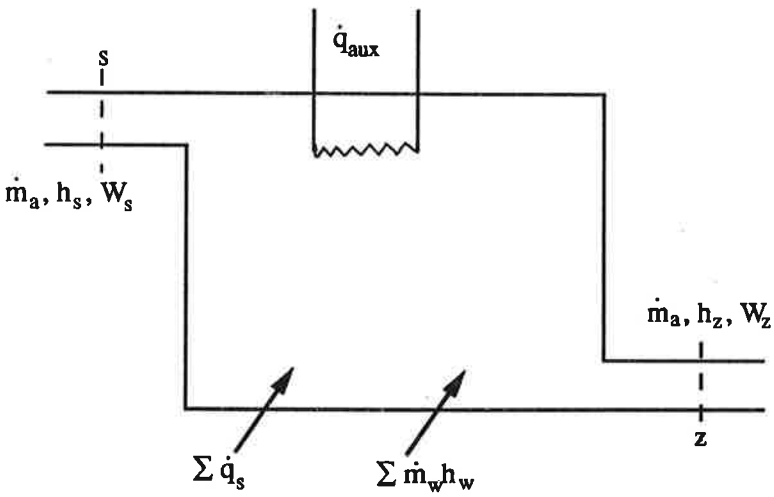

Figure 2 Enthalpy Balance on the Zone

where the rate of moisture removed from the supply air is equated to the moisture load on the zone. The enthalpy is related to dry bulb temperature (T) and humidity ratio (W). That is

$$h = Cp_a\ T + W\ (h_g + Cp_v\ T). \tag{3}$$

In SI units Equation (3) may be approximated as

$$h = T + W\ (2501 + 1.86\ T) \qquad \text{kJ/kg} \tag{4}$$

Equations (1) and (2) describe the energy and mass balance on the zone. However, as shown in Fig. 1, the condition of air is changing continuously while the air is circulated in the ductwork. For example, the enthalpy of the air must be computed i) just after the exhaust air damper, ii) at the mixing box, iii) after the cooling and dehumidifying coil and iv) after the fan. While the enthalpy is computed at the above mentioned points, allowance must be made for heat gains/ or losses all along the ductwork. Therefore, it is evident that models for i) cooling and dehumidifying coil, ii) the fan and iii) the ductwork are required. In the following, these models are briefly described together with a model for the chiller.

2.1.1 Cooling and Dehumidifying Coil Model

The cooling coil model developed in reference 8 was used. For simplicity the steady-state version of the model is used in this study. The cooling coil modeled is of counter-cross flow type with circular fins on the tubes. The model is capable of simulating different coil configurations such as varying the number of rows of tubes and the number of fins per unit length of tube. Given the inlet temperature of the chilled water T_w and the conditions of the air entering the coil, the leaving conditions of air from the coil are described by the following equations.

$$\frac{dT_a}{dy} = -\ C_1\,(T_a - T_{t,o}), \tag{5}$$

$$\frac{dW_a}{dy} = -\ C_2(W_a - W_{t,o,st}), \tag{6}$$

$$\frac{dT_w}{dx} = -\ C_3(T_w - T_{t,o}), \tag{7}$$

$$T_{t,o} = C_4\ [T_a + C_5\ T_w + C_6\ (W_a - W_{t,o,st})]\,, \tag{8}$$

and

$$W_{t,o,st} = 7.93x10^{-3} + 3.1x10^{-4}\, T_{t,o} + 7.5x10^{-6}\, (T_{t,o} - 53)^2. \qquad (9)$$

where

T_a is the air temperature
T_w is the water temperature
$T_{t,o}$ is the tube surface temperature
W_a is the humidity ratio of the air
$W_{t,o,st}$ is the humidity ratio at saturation.

The coefficients C_1 to C_6 are given by

$$C_1 = \frac{E_{s,ov}}{R_a\, m_a\, C_p}, \qquad (10)$$

$$C_2 = \frac{E_{c,ov}}{R_a\, m_a\, Le}, \qquad (11)$$

$$C_3 = \frac{1}{R_w\, m_w\, C_w}, \qquad (12)$$

$$C_4 = \frac{R_w\ E_{s,ov}}{R_a + R_w E_{s,ov}}, \qquad (13)$$

$$C_5 = \frac{R_a}{R_w\ E_{s,ov}}, \qquad (14)$$

$$C_6 = \frac{E_{c,ov}\ i_g}{Le\ C_p\ E_{s,ov}}. \qquad (15)$$

These coefficients are functions of the air-side and water-side resistances (R_a, R_w), efficiency of the fin ($E_{s,ov}$), mass flow rates of air (m_a) and water (m_w) and Lewis number (Le).

Equation (5) to (9) were solved for the temperature T_a and humidity ratio W_a of the air leaving the coil. The chilled water temperature was obtained by solving the chiller and storage tank model as follows.

2.1.2 The Chiller and Storage Tank Model

If T_w is the chilled water temperature and C_w is the thermal capacity of the storage tank, the energy balance on the tank is written

$$C_w \frac{dT_w}{dt} = - U_{1max}\, a_w\, (T_w - T_{wr}) - U_2 U_{max} (COP) + U\, A_w (T_\infty - T_w) \quad (16)$$

where the rate of energy stored in the tank is equated to the energy withdrawn from the tank, the rate of energy extracted from the water and the heat gains from the surroundings.

U_1 in Equation (16) is the mass flow rate of chilled water supplied to the cooling coil and U_2 is the input energy (control variable) to the chiller. The coefficient of performance of the chiller was modeled as

$$COP = P\left(1 - \frac{T_o - T_w}{\Delta T_{max}}\right) \quad (17)$$

where T_o is the sink temperature and ΔT_{max} is the maximum temperature differential the chiller is designed to work with.

2.1.3 The Fan Model

The heat generated by the fan motor is part of the cooling load. Therefore, it must be added as sensible heat gain to the air. The fan model given in reference 9 was used. The heat delivered to the air is expressed as

$$P_{fan} = P_{rated}\left(1.53x10^{-3} + 5.2x10^{-3}\ PLR + 1.11\ PLR^2 - 0.116\ PLR^3\right) \quad (18)$$

where

$$PLR = \frac{\text{Supply air flow rate}}{\text{Rated flow rate of the fan}}. \quad (19)$$

2.1.4 The Duct Model

Although transient models for duct heat loss or gain are available [10], a simple static model was used. The heat loss or gain from the duct was expressed as

$$q_{duct} = U\,A\,(\,T_a - T_\infty) \qquad (20)$$

where T_a is the air temperature and T_∞ is the temperature of the surrounding air. Apart from the models described above, a zone loads model is required in order to predict the sensible and latent loads on the zone. For this purpose a model developed in a previous study [11] was used. This is a transient model and is capable of predicting the sum of all the sensible heat loads (such as transmission loss, infiltration, solar and internal gains) and the latent loads. For simplicity output from the zone loads model [11] was used in this study. That is, the loads $\Sigma\, q_s$ and $\Sigma\, m_w\, h_w$ in Equation (1) were obtained from the zone loads model.

3.0 The Control Strategy

The control problem was broken down into two stages. First, the steady-state optimal control strategy was found using the techniques described in a previous study [12]. This steady-state optimal strategy was taken as reference and dynamic controllers of the form of modified lag compensators were designed to implement the steady-state optimal solution. We describe here the dynamic controller equations and a method of implementing them.

For simplicity only two controllers were implemented: namely, the settings for the coil face and bypass dampers (U_3) and the chiller input energy control (U_2) shown in Fig. 1. The controller equations were expressed as

$$U_2(n+1) = A\,U_2(n) + B\,K(n)\,[\,1 + T_w^* - T_w(n)\,] \qquad (21)$$

where A and B are constants, T_w^* is the optimal chilled water tank temperature and K is the dynamic gain factor. These are given by

$$T_w = T_s - \frac{Q_s + Q_l}{U_{1max} a_w \, E}, \qquad (22)$$

and

$$K(n) = \frac{U_{1max} a_w (T_w - T_{wr}) + U\, A_w (T_w - T_\infty)}{COP \;\; U_{2max}}. \qquad (23)$$

Similarly, the compensator algorithm for the coil face dampers was written

$$U_3(n+1) = C\, U_3(n) + D\, L(n)\, [\, 1 + h_s^* - h_s(n)\,] \qquad (24)$$

where

$$h_s^* = [\, T_s^* + W_s^* \,(\, 2051 + 1.86\, T_s^* \,)],\qquad (25)$$

$$T_s^* = T_{zset} - \frac{Q_s}{m_{aset} Cp}, \qquad (26)$$

$$W_s^* = W_{zset} - \frac{M_w}{m_{aset}}, \qquad (27)$$

$$L(n) = \frac{m_a \; [h_z(n) - h_s(n)]}{U_{1max} a_w (T_w - T_{wr})}. \qquad (28)$$

The air flow rates were computed a priori (it was assumed that an estimate of Q_s and Q_l are available) and thus the mass flow rate of supply air was obtained from

$$m_{aset} = \frac{Q_s + Q_l}{(h_{zset} - h_{sset})} \qquad (29)$$

3.1 Implementation Methodology

In order to implement the control strategy given by Equations (21) and (24), first the steady-state optimal values of h_s^* and T_w^* have to be calculated. One method of computing these values is to base them on estimated average loads. Since the actual zone loads are likely to be different from the estimated loads, the control algorithm tries to reduce the error between h_s^* and h_s, T_w^* and T_w.

On the other hand in order to calculate h_s and T_w, the model equations described in section 2 have to be solved. It was found that time steps between 3 to 12 minutes were adequate to ensure stable operation of the controllers.

4.0 Results and Discussion

Several simulation tests were carried out to study the time response characteristics of the controllers and as well as the typical daily operating performance. These results will be presented in two stages. First, the VAV system performance with only the face and bypass damper controller (U_3) in place will be given. In the second stage, the second controller (i.e. chiller input energy controller U_2) will be added and the overall performance of the VAV system when both U_2 and U_3 controllers are working will be discussed.

Shown in Figures 3a, b, c is the transient response of the coil face and bypass controller to a step input change in the total load (sum of the sensible and latent loads). The zone setpoint temperature was 23.8 C dry bulb (75 F) and the relative humidity was set at 50%. It may be noted from the figures 3a, b, c that as soon as the load is increased the controller opens the coil face dampers (Fig. 3a) and as a result the zone air temperature begins to decrease rapidly first (Fig. 3b) and gradually settles to a value close to the setpoint. The relative humidity as shown in Fig. 3c has settled to about 40% which is of course is less than the setpoint value. This is because of the temperature of the chilled water flowing in the coil which was set at a constant value corresponding to the maximum load. This has the effect of dehumidifying the supply air and thus the humidity level falls. However, a 40% relative humidity is still within the comfort zone. Also note that, the steady-state time of the controller seems to be about 30 minutes (from Fig. 3b the time required to reach within in ± 2% of the final value). This can be decreased somewhat by fine tuning the controller.

Figure 4a, b, c show the typical daily operating performance of the VAV system when only the face and bypass controller is working. The load profile for this day is shown in Figure 5. It may be noted from Figure 4b that the zone temperature is maintained close to the setpoint, however, the relative humidity is low during the peak load (between hours 9 to 18 as in Fig. 4b). The reason for this as pointed out earlier is that the temperature of the chilled water was assumed constant. This problem can be overcome by implementing the second controller (U_2) which can vary the chilled water temperature in response to the load variations. Also to note from Figure 4a is the fact that the face damper setting (U_3) is changing rapidly between 0 to 5 hours. This is attributed to the fact that the initial temperature of air was assumed arbitrarily which is likely to cause a large error between the zone air temperature and the setpoint. The controller therefore reacts to this large initial error as a result of which its response seems to be somewhat oscillatory. In terms of absolute values the temperature variation during this time is about ± 0.5 C which is not unreasonable.

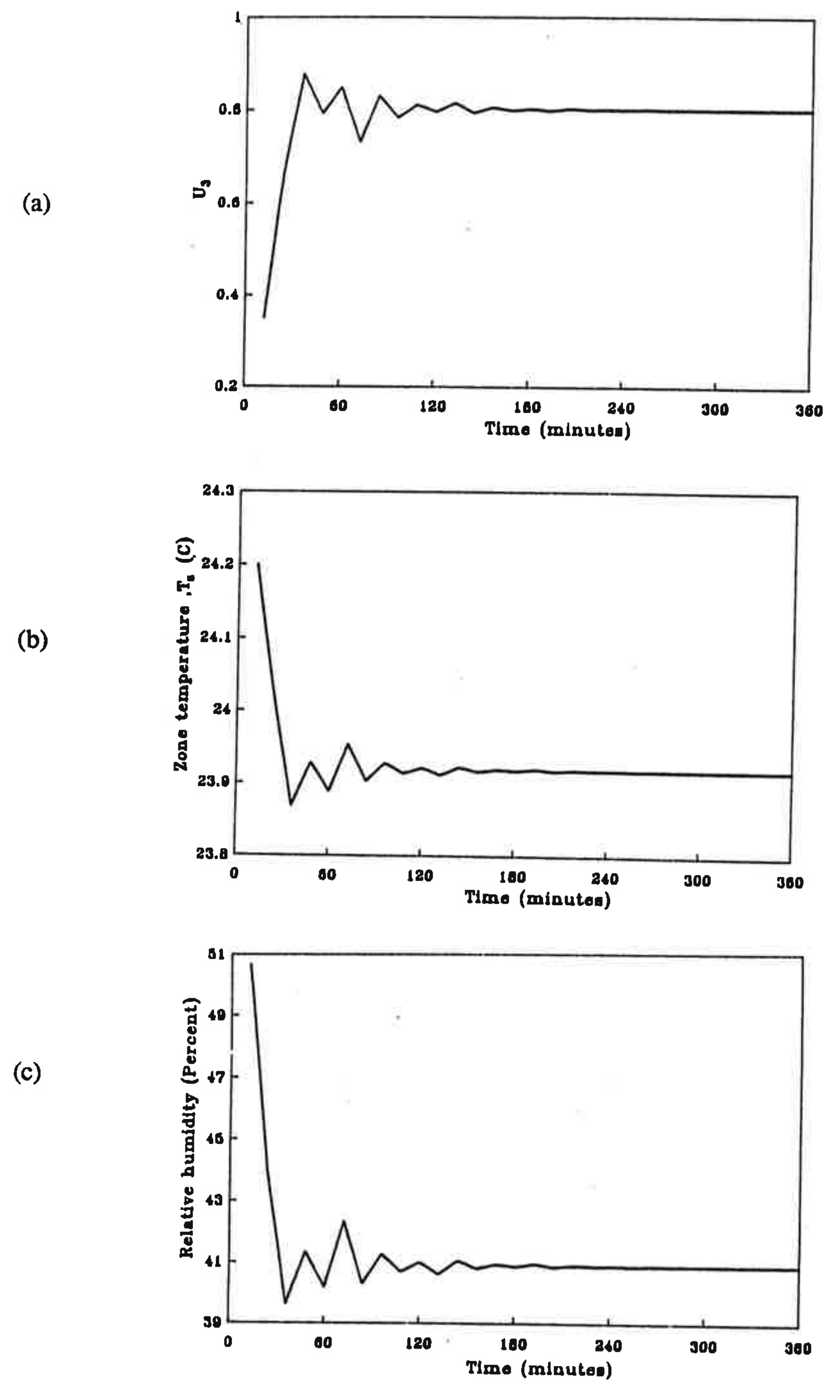

Figure 3 Transient response to a step input a) coil face damper opening fraction b) zone air temperature c) relative humidity.

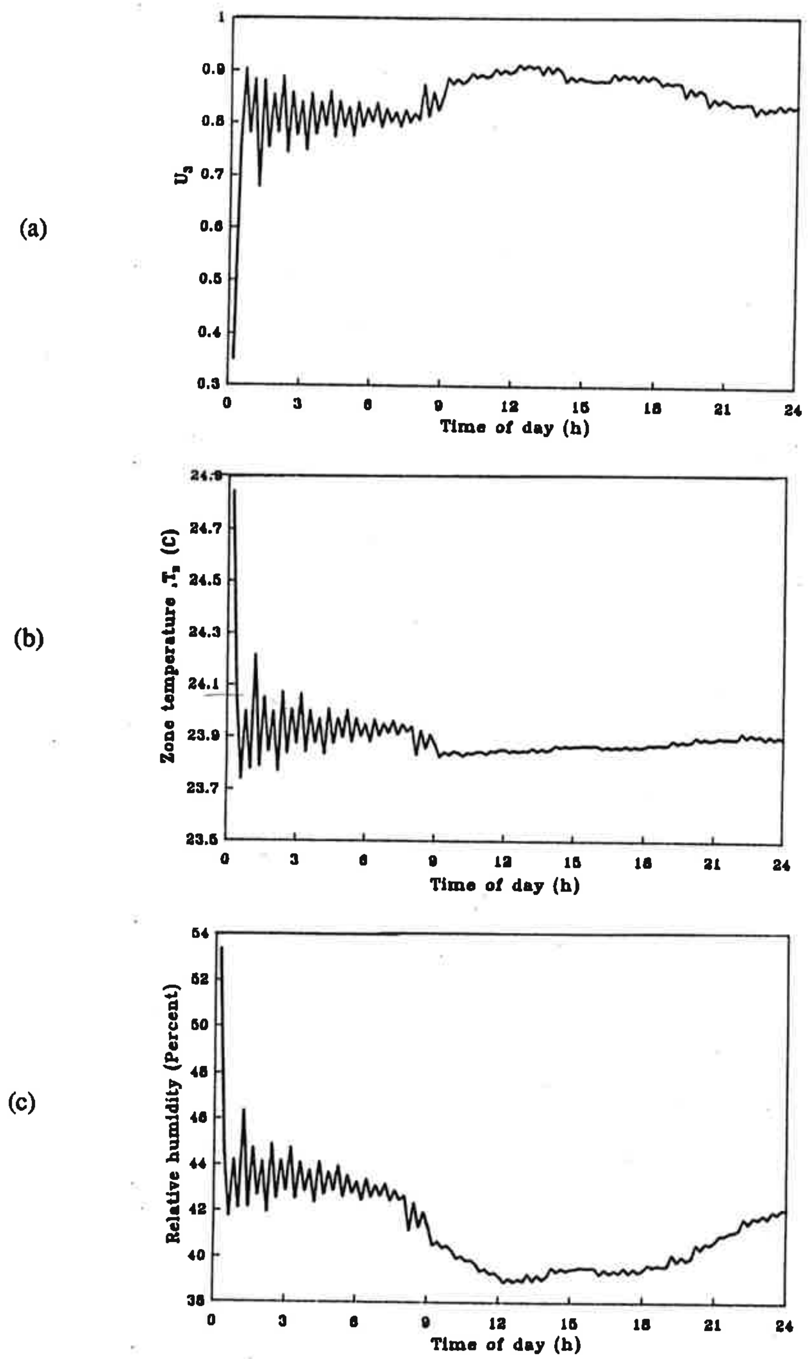

Figure 4 Typical daily response a) coil face damper opening fraction b) zone air temperautre c) relative humidity

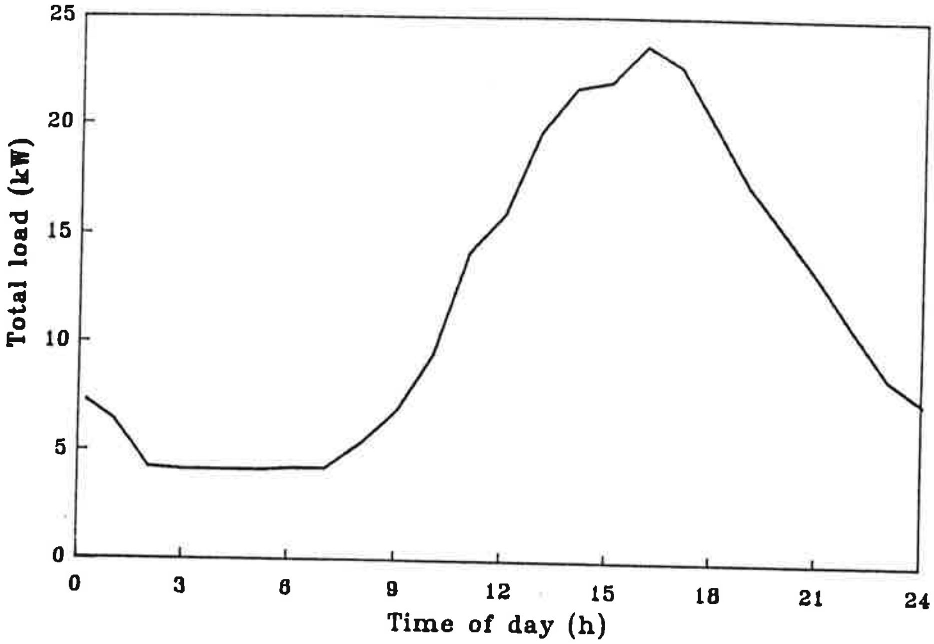

Figure 5 Typical daily load profile.

The VAV system performance can be further improved by implementing the second controller (U_2) for the chiller. In the following, the combined response of U_2 and U_3 controllers to changing loads will be discussed.

Figure 6a, b, c show the combined response of U_2 and U_3 controllers to a step change in load. Figure 6a shows that while the face damper opening fraction increases rapidly in response to the load, the chiller input energy is decreasing, suggesting that the chilled water from the storage tank is sufficiently low in temperature that it can be used directly in the coil while operating the chiller at very low levels to replenish the tank. The zone temperature is maintained very nearly at the setpoint (Fig. 6b). As far as the zone relative humidity is concerned the combined response of U_2 and U_3 has improved this value from about 40% as shown in Fig. 3c (when only U_3 was operating) to about 47% as shown in Fig. 6c (when both U_2 and U_3 are operating). This is a significant improvement given the fact that good humidity control is difficult to achieve in VAV systems.

Finally, the typical daily performance of the VAV system with both U_2 and U_3 controllers operating simultaneously is shown in Fig. 7a, b, c. The first thing to note from Fig. 7a is the fact that the chiller input energy increases during the peak hours (9 to 18 h) which is consistent with the load. The zone air temperature (Fig. 7b) and the relative humidity (Fig. 7c) are maintained close to

(a)

(b)

(c)

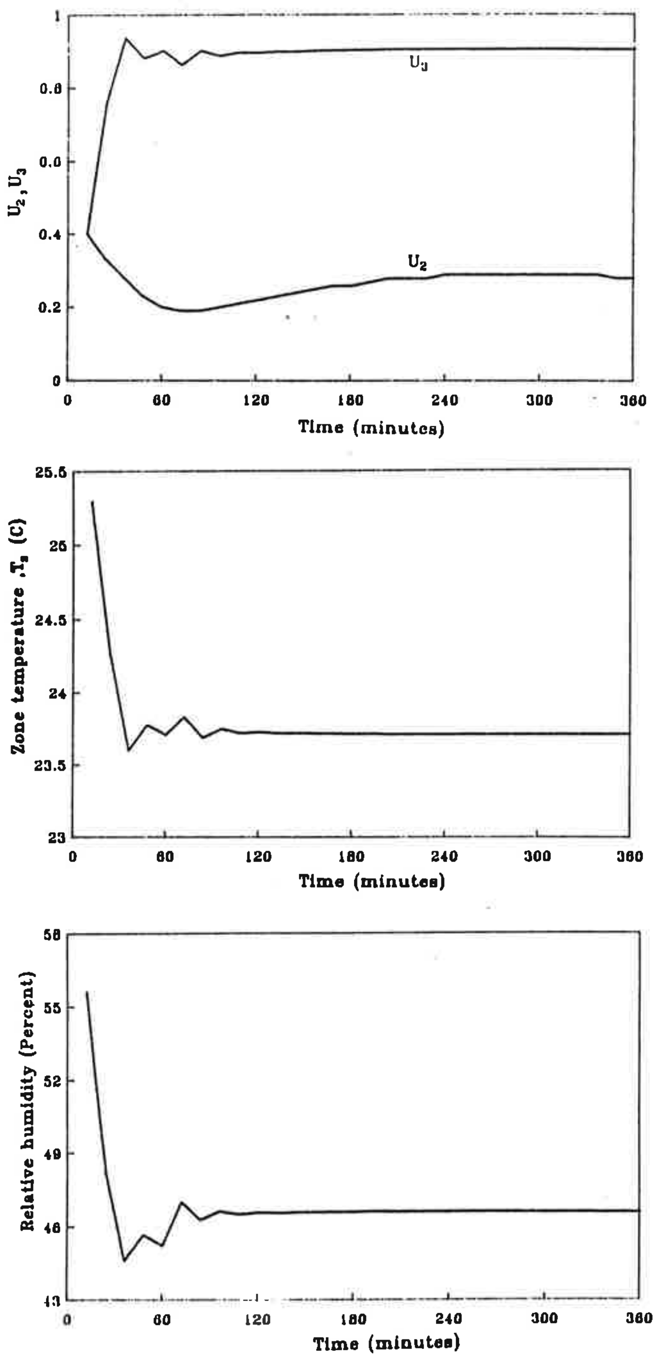

Figure 6 Time response to a step input when U_2 and U_3 are operated a) controller settings b) zone air temperature c) relative humidity

(a)

(b)

(c)

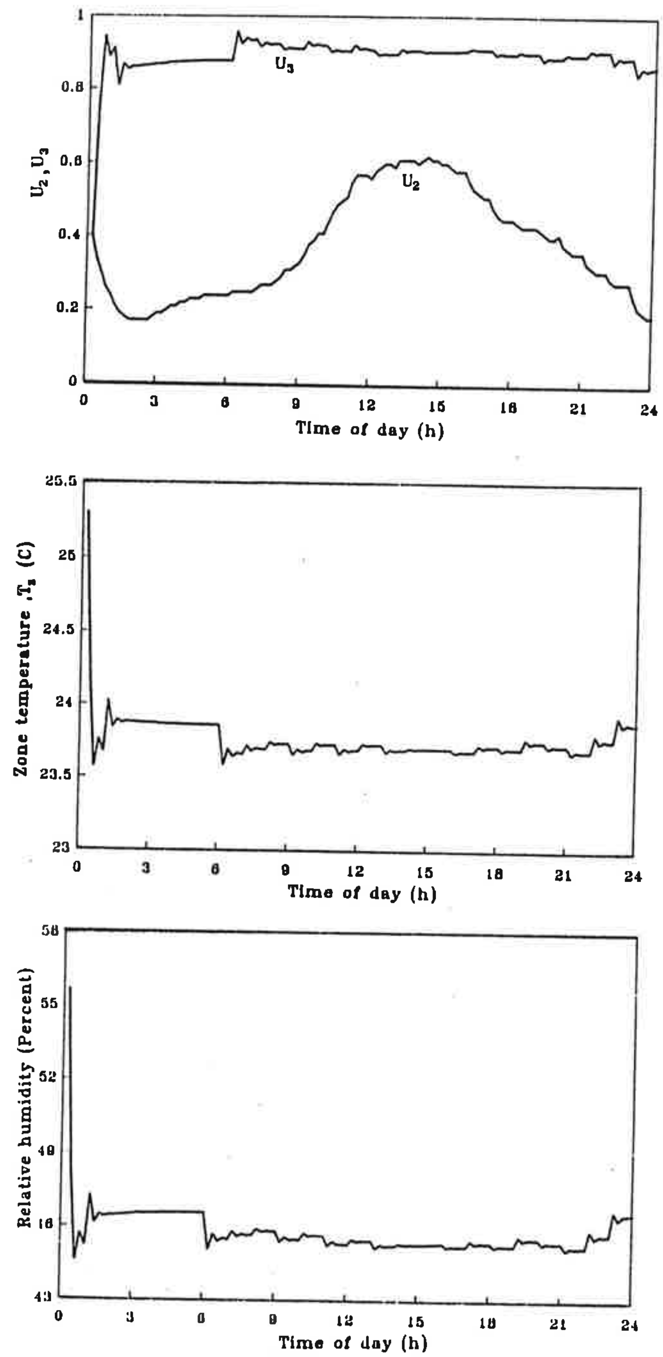

Figure 7 Typical daily response when both U_2 and U_3 are operated a) controller settings b) zone air temperature c) relative humidity

It must be pointed out here that the response of the controllers can be improved somewhat by fine tuning the parameters A, B, C and D in Equations (21) and (24). However, care must be taken to avoid oscillatory response which is likely to occur during sudden changes in loads. It was found that when the load variation is gradual, a value of A = B = 0.5 is satisfactory. On the other hand for rapidly changing loads, the magnitude of B has to be reduced while that of A has to be increased with A+B = 1.0. The same guide lines may be followed for choosing proper values of C and D.

5. Conclusions

A simple, implementable control strategy for a VAV system was developed based on two important considerations. It is assumed that an estimate of zone loads is available or can be predicted, and the steady-state optimal values for the reference inputs are precomputed based on the predicted loads. The implementation of the control strategy was achieved by developing a modified lag compensator which possess the capabilities of reducing the error between the steady-state optimal reference values (h_s^* and T_w^*) and the actual values h_s and T_w.

The time response characteristics of the controllers indicate that the control strategy is able to respond to the changing loads quickly and efficiently. This is evident from the fact that the interaction between the air-side (U_3) and the water-side (U_2) controllers is stable and their combined control action is such that the zone temperature and relative humidity are maintained close to the setpoint values.

Acknowledgements

This work was supported by grants from the Energy, Mines and Resources (EMR) Canada and the Natural Sciences and Engineering Research Council (NSERC) of Canada.

References

[1] F. C. McQuiston and J. D. Parker, "Heating, Ventilating, and Air Conditioning Analysis and Design", John Willey and Sons, 1988.

[2] L.K. Norford, A. Rabl and R.H. Socolow, "Control of Supply Air Temperature and Outdoor Air Flow and Its Effect on Energy Use in a Variable Air Volume System", ASHRAE Transactions, Vol. 92, Part 2B, 1986, pp. 30-45.

[3] G. Shavit and S.G. Brandt, "The Dynamic Performance of a Discharge Air-Temperature System with a P-I Controller", ASHRAE Transactions, Vol. 88, Part 2, 1982, pp. 826 - 838.

[4] D. P. Mehta, "Dynamic Performance of PI Controllers: Experimental Validation", ASHRAE Transactions, Vol. 93, Part 1B, 1987, pp. 1775 - 1793.

[5] C. G. Nesler and W. F. Stoecker, "Selecting the Proportional and Integral Constants in the Direct Digital Control of Discharge Air Temperature", ASHRAE Transactions, Vol. 90, Part 2B, 1984, pp. 834-845.

[6] S. G. Brandt, "Adaptive Control Implementation Issues", ASHRAE Transactions, Vol. 92, Part 2B, 1986, pp. 1- 8.

[7] R. H. Howell, "Variations in Relative Humidity in a Conditioned Space due to Coil Bypass Control Systems", ASHRAE Transactions, Vol. 92, Part 1B, 1986, pp. 499 - 508.

[8] A. H. Elmahdy, "Analytical and Experimental Multi-Row Finned-Tube Heat Exchanger Performance during Cooling and Dehumidification Processes", Ph. D dissertation, Carleton University, Ottawa, Canada, 1975.

[9] DOE -2 Engineering Manual, Version 2.1C, Lawrence Berkeley Laboratory, 1982

[10] R. A. Grot and D. T. Harrje, "Transient Performance of a Forced Warm Air Duct System", ASHRAE Transactions, Vol. 87, Part 1, 1981, pp. 795 - 804.

[11] M. Zaheer-uddin, "Sub-Optimal Controller for a Space Heating System", ASHRAE Transactions, Vol. 95, Part 2, 1989.

[12] H. Le, M. Zaheer-uddin, V. Gourishankar and R. Rink, "Near-Optimal Control of a Bilinear Solar-Assisted Heat Pump System", ASME Journal of Energy Engineering, Vol. 109, 1987, pp. 259 - 266.